Supplementary Material

Antagonistic mechanism of *Bacillus velezensis* HX0039 as a biocontrol agent against *Trichoderma virens*-induced 'Sanghuang' green mold

Ying Zhang[a,b,1], Wenheng Gao[a,b,1], Hui Zhang[a,b,1], Tao Sun[a,c], Huixiang Yang[a,b], Yan Liu[d], Xiaoyang Han[b], Dengke Yin[a,b,*], and Weifang Xu[a,b,¯]

[a] Joint Research Center for Chinese Herbal Medicine of Anhui of IHM, Anhui University of Chinese Medicine, Hefei, 230012, China

[b] Anhui Province Key Laboratory of Research and Development of Chinese Medicine, School of Pharmacy, Anhui University of Chinese Medicine, Hefei, 230012, China

[c] College of Life Science and Technology, China Pharmaceutical University, Nanjing, 211100, China

[d] Institute of Sericulture Science and Technology Research, Chongqing, 400700, China

¯Corresponding authors.

E-mail addresses: yindengke@ahtcm.edu.cn (D. Yin), xuweifang@ahtcm.edu.cn (W. Xu)

[1]These authors contributed equally to this work.

Table S1 Percentage of average nucleotide identity (ANI) between strain HX0039 and related *Bacillus* species.

Strain	GenBank No.	ANI%	GC content/%	Size/bp
Bacillus velezensis NJN-6	CP007165	99.91	46.55	4,052,546
Bacillus velezensis 19573-3	CP067043	99.40	46.56	3,990,203
Bacillus velezensis LF01	CP058216	99.35	46.56	3,974,023
Bacillus velezensis BY6	CP051011	99.41	46.61	3,898,273
Bacillus velezensis 160	CP119675	99.43	45.85	4,296,610
Bacillus velezensis QST713	CP025079	97.64	45.9	4,233,757
Bacillus velezensis SQR9	CP006890	97.63	46.1	4,117,023
Bacillus tequilensis EA-CB0015	CP048852	77.54	43.74	4,012,371
Bacillus subtilis BSD-2	CP013654	77.07	43.88	4,030,837
Bacillus subtilis 7PJ-16	CP023409	77.37	43.28	4,209,045
Bacillus licheniformis T5	CP124852	72.59	46.16	4,247,430
Bacillus licheniformis TAB7	CP027789	72.67	45.82	4,367,367
Bacillus pumilus SAFR-032	NC009848	70.91	41.29	3,704,641
Bacillus megaterium HGS7	CP065213	68.65	38.27	5,035,031
Bacillus megaterium WSH-002	CP003017	68.75	38.24	4,983,975
Bacillus megaterium QM B1551	CP001983	68.65	38.26	5,097,129
Bacillus cereus ATCC 14579	NC004722	68.08	35.28	5,411,809
Bacillus cereus AR156	CP015589	68.27	35.48	5,160,326
Paenibacillus polymyxa SQR-21	CP006872	65.92	45.64	5,828,436

Note: Taxonomic study of the bacterial strain HX0039 based on the most closely related bacterial strains belonging to closely related *Bacillus* sp. after average nucleotide identity (ANI) analysis. Species delineation thresholds were set at ANI values of 95%, which are widely accepted in microbial taxonomy for distinguishing bacterial species.

Table S2 General features of the strain HX0039 genome.

Features	Chromosome	Plasmid
Size(bp)	4,073,512	63,977
G + C content (%)	46.43%	41.84%
Number of CDSs	3,921	81
tRNA	82	0
rRNA	27	0

Note: CDSs represents protein-coding sequences.

Table S3 Overview of secondary metabolic gene clusters in the genome of *B. velezensis* HX0039 predicted by antiSMASH.

Region	Type	From	To	Similarity Confidence	Most similar known cluster
Region 1	NRPS,betalactone	10,812	148,640	High	fengycin
Region 2	transAT-PKS,NRPS,NRPS-like,T3PKS	203,233	313,356	High	bacillaene
Region 3	transAT-PKS	536,777	624,991	High	macrolactin H
Region 4	lanthipeptide-class-ii	788,966	817,85		-
Region 5	terpene	952,717	973,457		-
Region 6	PKS-like	1,055,480	1,096,724		-
Region 7	NRPS	1,626,712	1,692,119	High	surfactin
Region 8	NRPS,transAT-PKS	1,761,421	1,839,144	Low	locillomycin/locillomycin B/ locillomycin C
Region .9	other	2,318,397	2,359,815	High	bacilysin
Region .10	iPP-like,NRP-metallophore,NRPS,terpene-precursor	2,880,950	2,946,311	High	bacillibactin
Region 11	terpene-precursor	3,540,513	3,561,403		-
Region 12	transAT-PKS	3,584,720	3,690,886	High	difficidin
Region 13	terpene-precursor	3,751,532	3,772,581		-
Region 14	T3PKS	3,849,822	3,890,922		-
Region 15	terpene	3,999,059	4,020,942		-

Note: The symbol '-' indicates that no similar biosynthetic gene clusters (BGCs) were found. In this study, BGC similarity was determined by comparison against existing BGC entries in the "Minimum Information about a Biosynthetic Gene Cluster" (MIBiG) database.

NRPS = non-ribosomal peptide synthetase; PKS = polyketide synthase; transAT-PKS = trans-acyltransferase polyketide synthetases; T3PKS = type III polyketide.

Table S4 Gene statistics of predicted secondary metabolites detected in the genome of HX0039.

Metabolite	Gene name	Length/bp	Strain name (NCBI GenBank)
Fengycin	*fenA*	7,659	*Bacillus velezensis* FZB42 (CP000560.1)
	fenB	7,698	
	fenC	7,650	
	fenD	10,776	
	fenE	3,804	
	yngG	900	
	yngI	1,641	
Bacillomycin D	*bmyA*	11,949	*Bacillus velezensis* FZB42 (CP000560.1)
	bmyB	16,092	
	bmyC	7,860	
Iturin	*ituA*	11,939	*Bacillus subtilis* (AB050629.1)
	ituB	1,6089	
	ituC	7,857	
MacrilactinH	*pks2A*	2,307	*Bacillus velezensis* FZB42 (AJ634061.2)
	pks2B	12,261	
	pks2C	4,773	
	pks2D	8,739	
	pks2E	7,005	
	pks2F	5,721	
	pks2G	7,383	
Surfactin	*srfAA*	10,755	*Bacillus velezensis* FZB42 (AJ575642.1)
	srfAB	10,761	
	srfAC	3,837	
Lichenysin	*lchAA*	10,743	*Bacillus licheniformis* DSM 13 (AJ575642.1)
	lchAB	10,767	
	lch AC	3,849	
Bacillibactin	*dhbA*	786	*Bacillus subtilis subsp. subtilis str.* 168 (AL009126.3)
	dhbC	1,197	
	dhbF	7,137	

Note: The above genes originated from the Biosynthetic Gene Clusters (BGCs) located in regions 1, 3, 7, and 10 of antiSMASH prediction results.

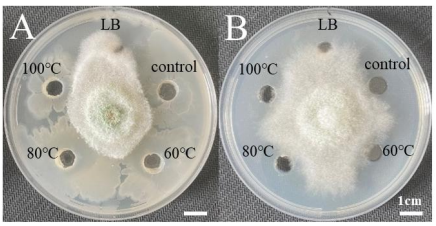

FIG S1 Antagonistic effects against *T. virens* SH4 of heat-treated HX0039 cell suspension (A) and cell-free supernatant (B). The mycelial disc of SH4 (5 mm) was inoculated in the middle of the PDA plate.

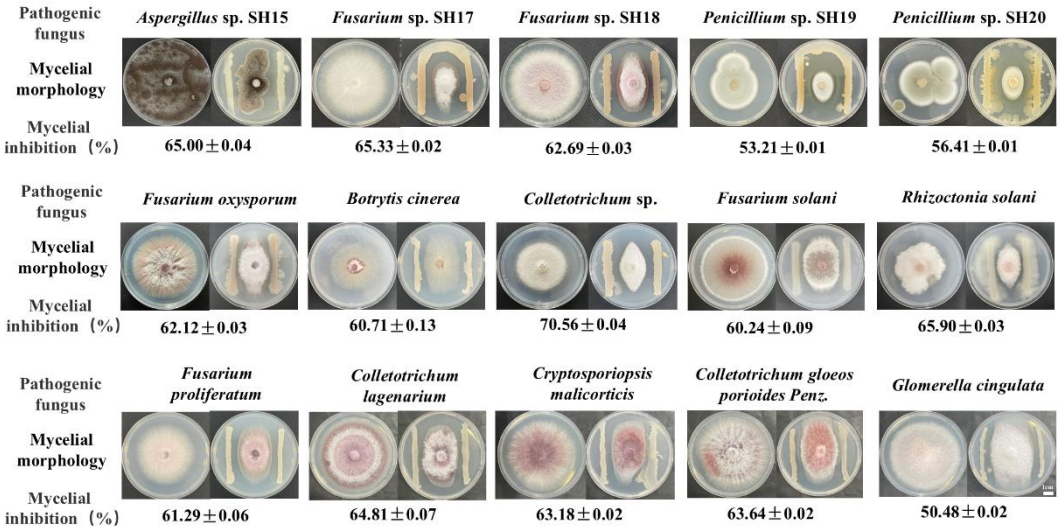

FIG S2 Antifungal activity of strain HX0039 against the selected pathogenic fungi. The left panel shows the control group, where a mycelial disc of the pathogenic fungus was inoculated onto a standard Potato Dextrose Agar (PDA) plate. In the right panel, the pathogenic fungus was inoculated at the center of a PDA plate, with the HX0039 cell suspension (10^8 CFU/mL) streaked on both sides. The mycelial inhibition rate (I) was calculated using the following formula: I (%) = [(the growth diameter of the fungal pathogen in the control group - the growth diameter of the pathogen in the HX0039 treatment plate)/(the growth diameter of the fungal pathogen in the control group-the diameter of the tested fungal agar disc (5.0 mm)] × 100

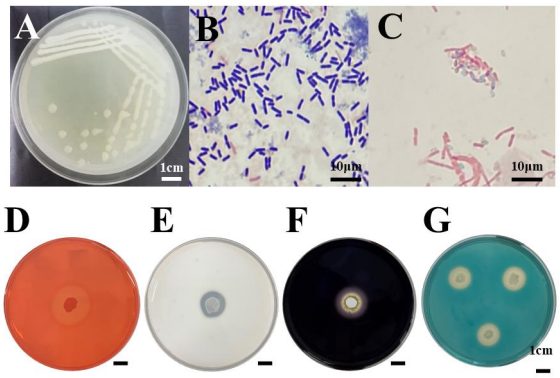

FIG S3 Morphological characterization and enzyme activity detection for strain HX0039. (A) Colony characteristics of strain HX0039 on LB after 24 h. (B) Gram staining. (C) Spore staining. (D) Cellulase detection. (E) Protease detection. (F) Amylase detection. (G) CAS plate detection the bacillibactin of strain HX0039. Note: LB=Luria–Bertani liquid medium

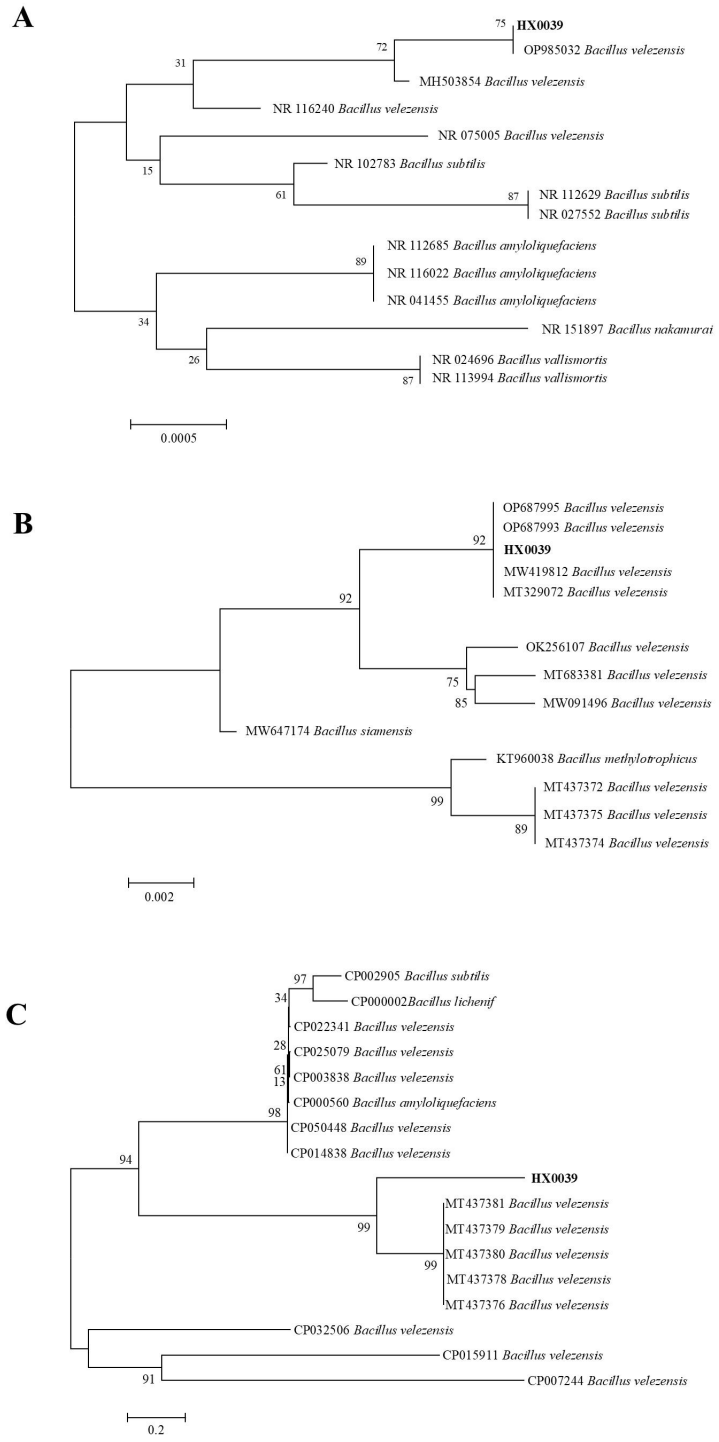

FIG S4 Phylogenetic trees of strain HX0039 based on 16S rRNA (A), *gyrA* (B) and *gyrB* (C) gene sequences. Phylogenetic trees were constructed using the neighbor-joining method in MEGA software version 7.0. Three separate phylogenetic trees based on each of the above single housekeeping genes were generated, with bootstrap values of 1000 replicates included for each tree.

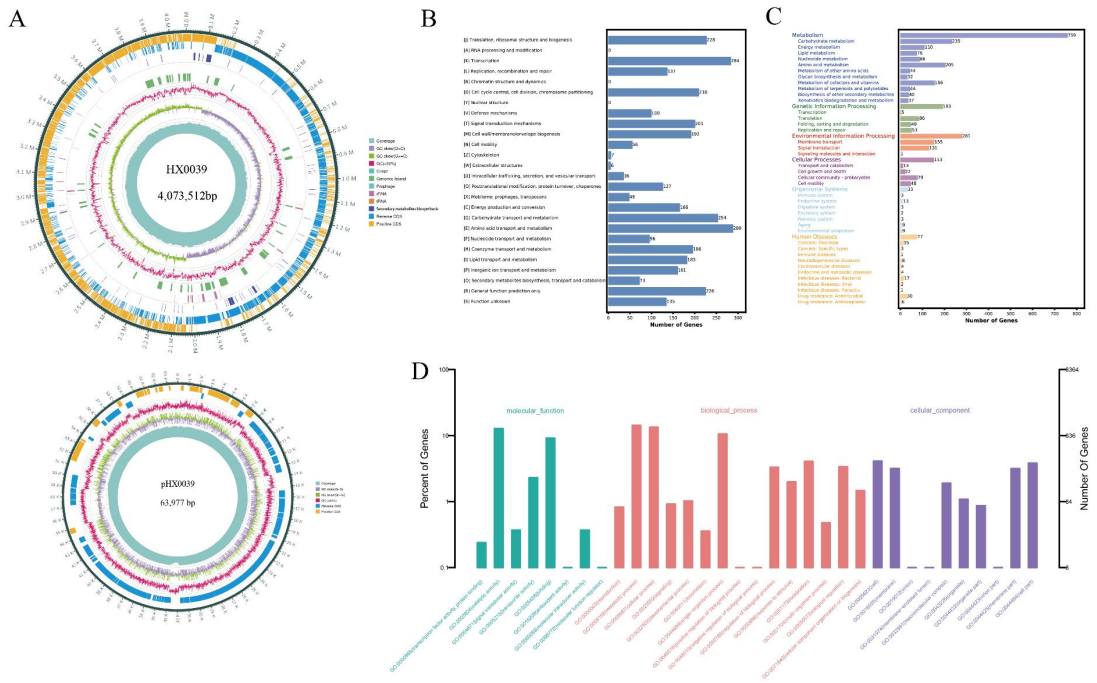

FIG S5 Genome maps of *B. velezensis* HX0039 and genome function annotation. (A) Circular maps of the chromosome and plasmid. The genomic circular diagrams from the outside to inside show the following: coding genes (righteous strand), coding genes (negative-sense strand), secondary metabolite gene density, tRNA (orange) and rRNA (purple), CRISPR, prophage and gene islands, GC ratio, GC skew, sequencing depth, plasmid circle map coding gene (righteous strand), coding gene (negative-sense strand), GC ratio, GC skew, sequencing depth. (B) Genome-encoded protein COG functional classification statistics. (C) KEGG functional classification statistics of genome-encoded proteins. (D) GO functional classification statistics of genome-encoded proteins.